

Temperature evolution from the $\delta^{18}\text{O}$ record of Hani peat, Northeast China, in the last 14000 years

HONG Bing^{1,2}, LIU CongQiang^{1†}, LIN QingHua¹, Shibata YASUYUKI³, LENG XueTian⁴, WANG Yu¹, ZHU YongXuan¹ & HONG YeTang¹

¹ State Key Laboratory of Environmental Geochemistry, Institute of Geochemistry, Chinese Academy of Sciences, Guiyang 550002, China;

² Graduate University of Chinese Academy of Sciences, Beijing 100049, China;

³ Environmental Chemistry Division, National Institute for Environmental Studies, Tsukuba, Ibaraki 305-0052, Japan;

⁴ College of Urban and Environmental Sciences, Northeast Normal University, Changchun 130024, China

From the last deglaciation to the Holocene, the Greenland Ice Core (GISP2) $\delta^{18}\text{O}$ records as well as the records of ice-rafted debris on the surface of the North Atlantic have revealed a succession of sudden cooling events on the centennial to millennial scales. However, the temperature proxy records are rarely studied systematically and directly to ensure that this air temperature cooling pattern simultaneously existed in the East Asian Region, in addition to the repeated pattern occurring in the Greater Atlantic Region. A peat cellulose $\delta^{18}\text{O}$ temperature proxy record proximately existing for 14000 years was picked up from the Hani peat in Jilin Province, China. It suggests by comparison that the sudden cooling events, such as the Older Dryas, Inter-Allerød, Younger Dryas, and nine ice-rafted debris events of the North Atlantic, are almost entirely reiterated in the temperature signals of Hani peat cellulose $\delta^{18}\text{O}$. These cooling events show that the repeatedly occurring temperature cooling pattern not only appeared in the North Atlantic Region in the high latitudes, but also in the Northwest Pacific Region in the middle latitudes. The climate change events marking the start of the Holocene Epoch, the Holocene Megathermal, the “8.2 kyr” event, the “4.2 kyr” event, the Medieval Warm Period, and the Little Ice Age are further discussed. The sensitivity response of Hani peat cellulose $\delta^{18}\text{O}$ to the land surface temperature and the reason for the age accuracy of peat cellulose ^{14}C are also discussed based on the characteristics of the peat bog environment.

Holocene, abrupt climate change, peat, Holocene Megathermal, 8.2 kyr event, 4.2 kyr event, Medieval Warm Period, Little Ice Age

Two important issues in paleoclimate research are the distribution of abrupt climate anomalies around the globe and their impact on regional social economic development. Researchers pay a special attention to large-scale sudden anomalous climates in different regions of the world and probe the teleconnection among those phenomena. At the same time, they also strive to determine the driving factors of global climates to study the mechanism of global climate change and to provide a foundation for evaluating current climate change and predicting future climate.

The sudden temperature decrease event from the late

deglaciation to the Holocene is an issue that has raised much concern. Since the 1960s, US and Western European scientists have been studying the Greenland icecap and the North Atlantic, finding that the temperature changes during the late deglaciation were unsteady and included a succession of sudden cooling events, such as the Older Dryas, Inter-Allerød, and Younger Dryas (YD). These phenomena were demonstrated through two re-

Received October 9, 2008; accepted January 15, 2009; published online June 10, 2009
doi: 10.1007/s11430-009-0086-z

†Corresponding author (email: liucongqiang@vip.skleg.cn)

Supported by National Natural Science Foundation of China (Grant Nos. 40573004, 40673069, 40231007)

search projects on the Greenland icecap, especially the ice core of the second Greenland icecap project (GISP2) $\delta^{18}\text{O}$. For the Holocene, GISP2 $\delta^{18}\text{O}$ showed a relative stability, although one record revealed clearly that a dramatic temperature decrease event occurred at 8.2 ka BP^[1]. On the contrary, the ice-rafted debris (IRD) record of the North Atlantic Ocean clearly indicates nine oceanographic and atmospheric cooling events during the Holocene. However, for the late deglaciation, the information provided by the IRD records is much less detailed than that provided by GISP2 $\delta^{18}\text{O}$ records^[2,3]. The question that arises from these data is whether or not the sudden temperature anomaly recorded respectively by the two climate proxy records during this long period reflects a kind of universal rule. In other words, does this kind of repeatedly seen temperature anomaly model also exist simultaneously beyond the Greater Atlantic Region, especially in the East Asian Region? These questions demand an answer. Previous work in the East Asian Region has detected a precipitation anomaly teleconnected with some of the temperature anomalies mentioned above, using proxy records such as precipitation^[4–7]. In fact, some temperature proxy records even suggested that one or some of the above-mentioned temperature anomaly events had occurred in East Asian Regions. Nevertheless, the data still fall short and there is a need for a systematic contrast study of this kind of repeatedly occurring temperature anomaly relative to a sensitive temperature proxy record.

This paper assesses information about land surface temperature from a time sequence of Hani peat cellulose spanning approximately 14000 years and reconstructs the evolution of land surface temperature in the Northwest Pacific Region from the late deglaciation to Holocene. The goal was a better understanding of the temperature evolution process of the region and the teleconnection between this process and the temperature change at high north latitude. The results reveal the basic characteristics of the land surface temperature evolution from the late deglaciation to the Holocene and provide a historic background for a better understanding of the current climate change in contrast with such records as GISP2 $\delta^{18}\text{O}$ and the IRD of the North Atlantic as well as historic materials.

1 Study region

The research site for the work was in a peat land in the Hani village of Liuhe County, Jilin Province (42°13'N, 126°31'E), with an altitude 900 m above sea level (Figure 1). It is a valley peat bog situated on the west piedmont of the Changbai Mountain peak and the middle part of the Longgang Mountain Chain in the Changbai Mountain region of northeastern China. The regional landform features are the Xuanwu lava plateau as well as eroded and denuded middle–low mountains rising and falling slightly. The peat land developed in the late Pleistocene Nanping period on the low-lying valley located in the Hani and dammed by the effusive mass of the volcano^[8]. The region belongs to the temperate continental monsoon climate, with 5.5°C as the approximate annual average temperature, and about 20°C as the monthly average temperature from June to August. The frost period lasts for around 250 days and the freezing period is over half a year (from November to the April of the following year). The summer precipitation is mainly influenced by moisture brought by the East Asian monsoon^[5]. The summer is wet and rainy whereas the autumn is moderate and cool with an annual precipitation of about 750 mm.

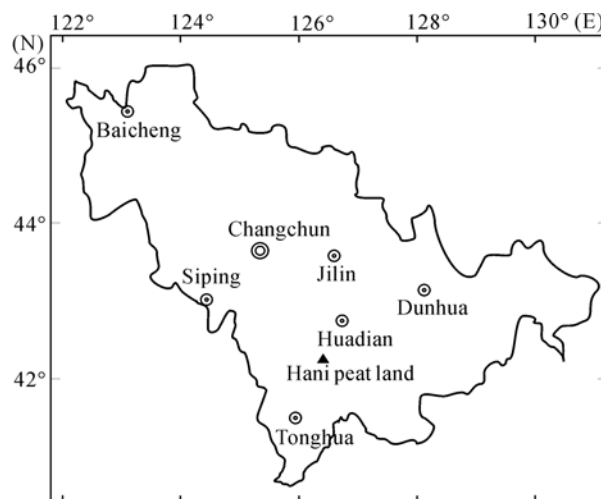


Figure 1 Sketch map showing the location of the research site.

2 Materials and methods

A peat column composed of continuous herbaceous peat was drilled into the thick layer deposit zone located in the northern side of the Hani peat land with an improved Russian Peat Corer. Apart from the grass-root layer of

about 0.4 m on the top, the length of the peat column was about 8.78 m. A total of 878 peat sub-samples were obtained by cutting the column at an interval of 1 cm. The modern plant growth status on the peat land was investigated, and 18 types of common plant samples were collected. Cellulose was extracted from the modern plants and peat plant residues by the sodium chlorite oxidation method with our improved protocol^[4,9].

Cellulose is the most abundant organic substance in plants and is a macromolecule polymer of interlinked dextroglucose molecules. It can be divided into different types such as α , β and γ , depending on its structure. Cellulose in plants mainly belongs to α -cellulose and other types such as β cellulose are negligible. Plant cellulose has two important features. First, the isotopic composition of the hydrogen, carbon, and oxygen molecules linked on the cellulose carbon chain will undergo no further change in the decomposition process after the death of plants^[10]; thus, information about the climatic environment at the time the cellulose was generated is retained. Second, along with the photosynthesis of plants and the generation of cellulose, the radioactive ^{14}C molecules in the air at that time also are coupled onto the cellulose, again preserving information from the generation time of the cellulose; thus, the radioactivity intensity of cellulose ^{14}C contains information that directly indicates the air environmental conditions. Plant cellulose therefore serves as a potential biomarker to indicate climate change. In addition, two problems can be clarified based on the paleoclimate information provided by the peat plant cellulose, as described below.

The first problem is the relationship between the oxygen isotope composition of peat cellulose and the land surface temperature. As recently observed^[11], since the discovery in the 1940s of the relationship between the $\delta^{18}\text{O}$ of annual tree rings and the land surface temperature, changes in $\delta^{18}\text{O}$ during plant soil absorption have been studied. This research has revealed that there is no large fractionation from the $\delta^{18}\text{O}$ of the plant and that the $\delta^{18}\text{O}$ of the source water has a great impact on that of the plant^[12,13]. Therefore, the $\delta^{18}\text{O}$ of plant tissue reflects that of the source water, thus indirectly reflecting the temperature at that point of time^[11]. Libby et al.^[14] proposed in 1976 that the $\delta^{18}\text{O}$ of annual tree rings could therefore be used as an "isotope thermometer"^[14]. The $\delta^{18}\text{O}$ of plant tissue is also influenced by other factors like relative humidity and has successfully been

applied to elucidate precipitation evolutionary history^[11,15–17]. In recent years, researchers have tried to simplify the model that influences $\delta^{18}\text{O}$ and to apprehend the quantitative relationship between the $\delta^{18}\text{O}$ of plant cellulose and that of the source water to infer a quantitative temperature evolution^[18].

Peat is obviously different from tree rings because of its special environment and its composition of various plants. Swamp vegetation dominated by the sedge family plants is formed because of swamp environmental conditions favoring the development of the peat^[19]. Furthermore, the peat deposit of some thick layers on the Chinese mainland always develops in relatively stable sedimentary environments like long-standing subsidized areas (such as Ruergai at the eastern edge of the Tibetan Plateau and the Hongyuan peat) in geological history, or a crater lake (Jinchuan peat in Jilin Province), or a dammed lake (Hani peat in Jilin Province); thus, the floristic composition is relatively stable in term of the peat profile. The importance of the relative stability of the floristic composition was highlighted in particular during the study of Jinchuan peat, which revealed that more than 80% of the plant residue on the profile was composed of vascular sedge family plants with a similar model of water use, while the peat moss flora residue took up an extremely small proportion (Figure 2 of ref. [20]). Located in the southeast, Hani peat land is about 15 km from the Jinchuan peat land, which belongs to the middle–low mountain bioclimatic zone, and the peat profile is mainly composed of the vascular sedge family plants. The test results of the $\delta^{18}\text{O}$ values of 18 common plant celluloses in the Hani peat land further revealed that apart from a single unusual and unexplained value (*Carex*), the $\delta^{18}\text{O}$ values for the remaining 17 plants were in close proximity to each other, with an average value of $20.9\text{‰} \pm 0.3\text{‰}$ (Table 1). Among these, the $\delta^{18}\text{O}$ average value of *Eriophorum vaginatum* and *Carex tenuiflora* was $21.4\text{‰} \pm 0.0\text{‰}$, and the $\delta^{18}\text{O}$ average value of the remaining 15 plants was $20.5\text{‰} \pm 0.0\text{‰}$. As a result, as was the case with the Jinchuan peat, the impacts of the different plants on the profile of Hani peat composition and change are small, while the responses of $\delta^{18}\text{O}$ of different plants to the land surface temperature are almost the same.

The sensitivity response of the peat plant cellulose $\delta^{18}\text{O}$ to the land surface temperature stems from its special swamp ecological environment. Peat lands such as

Table 1 Oxygen isotope composition of modern plants in Hani peat land

No.	Plant name	$\delta^{18}\text{O}$ (‰, VSMOW)	Std. (‰)
HN1	<i>Sphagnum palustre</i>	19.89	$\leq \pm 0.6$
HN2	<i>Sphagnum magellanicum</i>	20.58	$\leq \pm 0.6$
HN3	<i>Sphagnum acutifolium</i>	20.53	$\leq \pm 0.6$
HN4	<i>Polytrichum commune</i>	21.07	$\leq \pm 0.6$
HN5	<i>Calliergonella cuspidata</i>	20.70	$\leq \pm 0.6$
HN6	<i>Eriophorum vaginatum</i>	21.89	$\leq \pm 0.6$
HN7	<i>Carex schmidtii</i>	25.41	$\leq \pm 0.6$
HN8	<i>Carex tenuiflora</i>	20.97	$\leq \pm 0.6$
HN9	<i>Phragmites communis</i>	21.56	$\leq \pm 0.6$
HN10	<i>Typha latifolia</i>	20.83	$\leq \pm 0.6$
HN11	<i>Equisetum heleocharis</i>	20.53	$\leq \pm 0.6$
HN12	<i>Comarum palustre</i>	21.80	$\leq \pm 0.6$
HN13	<i>Larix olgensis</i>	20.16	$\leq \pm 0.6$
HN14	<i>Betula ovalifolia</i>	19.40	$\leq \pm 0.6$
HN15	<i>Vaccinium uliginosum</i>	20.16	$\leq \pm 0.6$
HN16	<i>Ledum palustre</i> var. <i>dilatatum</i>	20.83	$\leq \pm 0.6$
HN17	<i>Ledum palustre</i> var. <i>angustum</i>	20.78	$\leq \pm 0.6$
HN18	<i>Chamaedaphne calyculata</i>	19.83	$\leq \pm 0.6$

Hani, Jinchuan, and Hongyuan are all swamp environments, and the ground is covered by snow and ice in autumn and winter. When the snow and ice melt into water in spring, and with the monsoon precipitation in summer, the ground is over-wet all year or covered by a thin layer of seep. This kind of swamp environment leads to the shallow attachment of the root system of herbaceous plants into the earth with little impact imposed by the deep groundwater; thus, the $\delta^{18}\text{O}$ of plants may depend more on the $\delta^{18}\text{O}$ of precipitation. More importantly, it also creates one of the necessary and major features for the peat swamp environment, i.e., the perennial wet microclimate makes the relative humidity of the air close to the surface of the swamp relatively significant and stable^[19,21]. Therefore, changes in the peat swamp plant cellulose $\delta^{18}\text{O}$ mainly stem from changes in $\delta^{18}\text{O}$ of the source water that the plants use, i.e., the precipitation. There is a close correlation between the $\delta^{18}\text{O}$ changes in precipitation and the air temperature changes^[22–24], and they are the mixtures of rainwater together with melt-water of snow and ice. Thus, the $\delta^{18}\text{O}$ of peat swamp plant cellulose could serve qualitatively as a proxy indicator for average annual temperature.

The above viewpoint is also supported by some measurement results. In 2002, Ménot-Combes et al.^[25] delivered their research findings on 13 peat lands in Switzerland, pointing out that the $\delta^{18}\text{O}$ of the surface water of these swamps closely correlated with that of the

precipitation; the water used in plant photosynthesis in the peat land reflected the isotope composition of the annual average precipitation. For most of the peat plants, especially the *Eriophorum vaginatum* and the *Sphagnum capillifolium* of the moss family, their cellulose $\delta^{18}\text{O}$ changes were mainly dominated by the oxygen isotope composition of precipitation. This finding highlights the importance of specific kinds of plants grown in the peat land to the paleoclimate restoration^[25].

The second problem that can be clarified based on the paleoclimate information provided by the peat plant cellulose is the age of cellulose ^{14}C in the peat sedimentary profile. The habit of plant root systems of always growing downwards may give rise to the question of whether the age of ^{14}C at any point on the profile decreases because of the downward penetration of its upper root systems. The truth is that the influence is slight for the following three reasons.

First and the most important, as mentioned above, many investigations have indicated that the majority of plant population in the peat swamp of Chinese mainland includes *Carex*, *Eriophorum vaginatum*, sedge and *Kobresia*^[19]. In the seep environment and under a corresponding climate, these plants show “unusual” growth characteristics to adapt to the hypoxic environment. Their curving subterranean stems tiller upwards and new roots come out; meanwhile, exiguous adventitious roots develop from these tiller roots to obtain more oxygen^[19]. With the growth of the plants year after year, the tiller roots move upwards slowly and form dense gilgai or

“tower heads.” The original subterranean stems and tiller roots are the main body forming the accumulation of persistent organic substances in the peat^[19]. The dense gilgais gradually extend to each other and finally develop new peat layers (Figure 2). Experts on peat lands think that “this physiological and ecological feature accounts for the development of the herbaceous peat”^[19]. It may form the hair-like bedding structure that is visible on the peat profile and also clarify the old to new sedimentary sequence principle on the peat profile from the lower part to the upper.

Second, as pointed out in previous research, the tiller roots of plants like *Carex* could come together to form a dense ecological feature. Thus, such plants would have a great impact on the development of peat. Aquatic plants and hygrophytes are not the main components of herbaceous peat. The majority of plants are those with abundant tiller roots and are better adapted to the hypoxic, low-nutrient, acidic swamp environment^[19]. As a result, because of the minority of other plant species, any influence from root systems growing downwards is limited. From the entire peat profile, the influence of the perennial and minor younger ¹⁴C brought by the root systems growing downwards is only a small systematic error added to the continuous age of ¹⁴C formed by the comparatively large quantity of tiller roots; this value should be within the error scope of modern ¹⁴C age test-

ing technology.

Third, in the process of field sampling and indoor pretreatment of the peat samples, the megascopic residual roots with root diameters more than 1 mm will be picked out first because they are always thick roots with deep penetration of some perennial woody plants. This procedure may effectively control the influence from root penetration.

To determine the $\delta^{18}\text{O}$ of the Hani peat cellulose, 200 μg of α -cellulose samples were weighed accurately and loaded into a silver capsule. After being dried in a vacuum system, the sample in the capsule was measured using continuous flow mass spectrometry (GV Instruments (Thermo Electron Corporation)). Of the 878 peat sub-samples, we stochastically assigned 439 sub-samples as the test samples. Parallel measurement for each of the total 439 sub-samples was carried out. In addition, we inserted a standard International Atomic Energy Agency sample of known oxygen isotope composition at an interval of 5–10 samples among the test samples to monitor and correct the quality of the test results. The standard deviations of all of the parallel measurement results were less than $\pm 0.6\text{‰}$.

To establish the ¹⁴C age framework, we first described the properties of the peat column samples collected on the field sampling spot and subdivided the column samples into several small fractions according to the color



Figure 2 The tiller roots move upwards slowly and form dense gilgai or “tower head”. (Ruergai peat land, east edge of Tibetan Plateau). The dense gilgais gradually extend to each other and finally develop new peat layers.

and texture changes of the fresh peat samples. The color and texture of each small fraction were the same; thus, correspondingly, the sedimentary environment and accumulative speed of each small fraction should be the same. Then we set up a ^{14}C age control point at the junction of two small column samples and added one ^{14}C age control point in some thicker small fractions of the column sample. Finally, a total of 13 ^{14}C age control points were set up (Figure 3). The peat cellulose sample of the control point was prepared with graphite targets, and their ^{14}C intensity was determined in the AMS Laboratory of the National Institute for Environmental Studies in Tsukuba, Japan, to obtain ^{14}C age; chronological age was obtained after correction using the CALIB-4.3 programme^[26]. We then obtained the chronological age se-

quence of the ^{14}C of Hani peat profile via the linear interpolation method. Of the 13 ^{14}C age data obtained (Table 2), 10 age data from the upper portions that were 7.45 m long have been published in a previous work regarding the climate proxy records of Hani Peat $\delta^{13}\text{C}$ and the East Asian Monsoon evolutionary history^[5].

3 Results and discussion

3.1 Temperature anomalies of the last deglaciation

The $\delta^{18}\text{O}$ time series of Hani peat cellulose (Figure 4(b)) provides a continuous proxy record for surface air temperature changes during the period from the last deglaciation through the Holocene. Its general evolution conforms to the trend integrated by several proxy re-

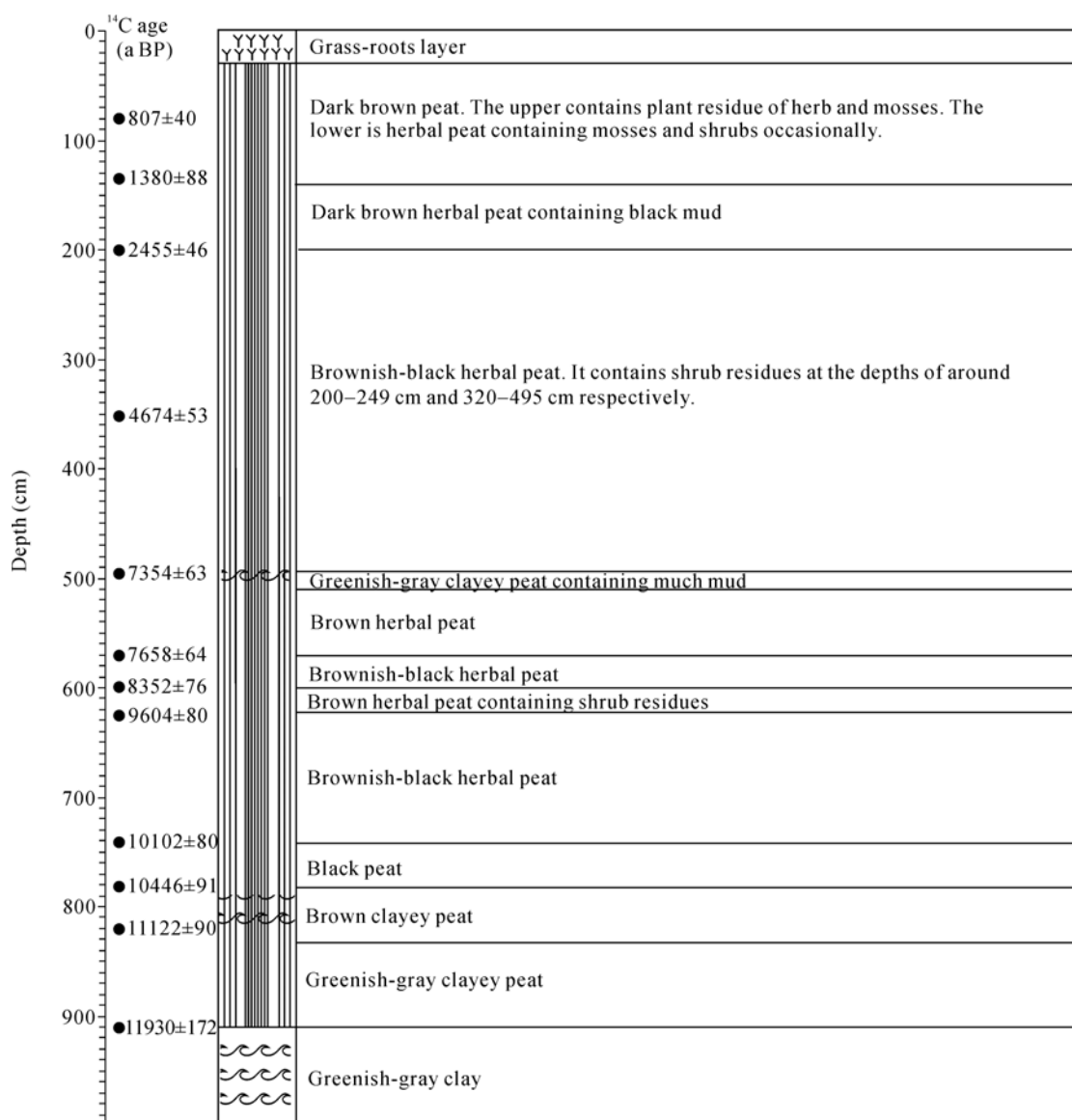


Figure 3 Color and qualitative characteristics of fresh peat core from Hani peat bog.

Table 2 Radiocarbon dates of Hani peat profile

No.	AMS sample depth (cm)	$\delta^{13}\text{C}$ (‰, VPDB)	AMS ^{14}C age (^{14}C yr BP)	Calibrated age 1σ (cal. yr BP)
HA2	80	-26.10	807±40	722
HA3	135	-26.78	1380±88	1292
HA4	200	-25.81	2455±46	2673
HA5	350	-26.22	4674±53	5383
HA6	495	-26.97	7354±63	8171
HA7	570	-27.98	7658±64	8412
HA8	600	-27.02	8352±76	9337
HA9	625	-26.84	9604±80	10745
HA10	740	-27.13	10102±80	11643
HA11	745	-26.94	10399±89	12336
HA12	780	-26.53	10446±91	12356
HA13	820	-26.27	11122±90	13135
HA14	900	-27.43	11930±172	13937

cords internationally (Holocene climatic optimum—<http://www.mirrorin.com/wikipedia>). Comparison with both the GISP2 $\delta^{18}\text{O}$ record (Figure 4(a)) and the ice-rafted record of the North Atlantic (Figure 4(c)) shows that the Hani $\delta^{18}\text{O}$ record comprehensively replicates almost all of the century-millennial timescale's abrupt temperature anomalies inferred respectively from each of the other records. First, like the GISP2 $\delta^{18}\text{O}$ record, the Hani $\delta^{18}\text{O}$ record reveals three abrupt warming and three abrupt cooling events in the last deglaciation. An amplitude maximum value of the Hani $\delta^{18}\text{O}$ during about 14.2 to 14.1 cal. kyr BP indicates the first warming event in the last deglaciation, corresponding to the late period of the Bølling warming event that occurred during about 14.6 to 14.1 cal. kyr BP in the GISP2 $\delta^{18}\text{O}$ record^[1]. Subsequently, Hani $\delta^{18}\text{O}$ suddenly decreased, indicating the occurrence of the Older Dryas event. This cooling event lasted around 200 years, a longer interval than the Older Dryas indicated by the Greenland $\delta^{18}\text{O}$ record. Starting from around 13.9 cal. kyr BP, Hani $\delta^{18}\text{O}$ suddenly increased again and reached its peak value at around 13.8 cal. kyr BP, indicating the beginning of the Allerød warming event. The terminal time of the Allerød event inferred from both the GISP2 and the Hani $\delta^{18}\text{O}$ records is around 13.0 cal. kyr BP^[1]. Both the Hani and the GISP2 $\delta^{18}\text{O}$ records indicate that the Allerød was clearly colder than the Bølling, which is the reverse of inferences drawn from European and North African $\delta^{13}\text{C}$ stalagmite profiles^[27]. An abrupt decrease of the Hani $\delta^{18}\text{O}$ at around 13.5 cal. kyr BP shows that the Allerød warming phase was unstable and was interrupted by the so-called Inter-Allerød cold event, which is also observed in the GISP2 $\delta^{18}\text{O}$ record^[1].

Starting from around 12.9 cal. kyr BP, Hani and GISP2 $\delta^{18}\text{O}$ values both suddenly decreased, indicating the onset of the YD event, the most notable cooling event in the last deglaciation. This temperature drop may have lasted around 300 years and at around 12.6 cal. kyr BP reached its lowest value over the past 14.2 kyr. After this, the Hani and GISP2 $\delta^{18}\text{O}$ values both increased gradually, reaching a peak of around 12.0 cal. kyr BP. This phenomenon reveals that climatic conditions underwent amelioration during the middle YD event, which had been construed as a warm event because at this time the $\delta^{13}\text{C}$ amplitude of the European stalagmite was almost half that of the YD onset^[27]. After this warming process, both the Hani and the GISP2 $\delta^{18}\text{O}$ decreased again, and the YD event ended at around 11.7 cal. kyr BP^[1].

3.2 The beginning of the Holocene and the Holocene Megathermal

The opening time of the Holocene epoch is unclear. It is commonly thought that the Holocene may start from a strong warming process. However, based on the comparison between Hani, GISP2, and ice-rafted records, an abrupt cooling event following YD event would be considered as a clear sign for the beginning of the Holocene. Figure 4B shows that at about 11.6 cal. kyr BP the Hani $\delta^{18}\text{O}$ decreased again suddenly after a short increase following the end of the YD event; at the same time, a clear ice-rafted debris (IRD) event (IRD 8) occurred in the North Atlantic (Figure 4(c)). The signal for a sudden temperature drop is also visible in the GISP2 $\delta^{18}\text{O}$ record (Figure 4(a)). After this cooling event a strong warming process could have overcome the influence on the Earth's climate of the last deglaciation. Nevertheless,

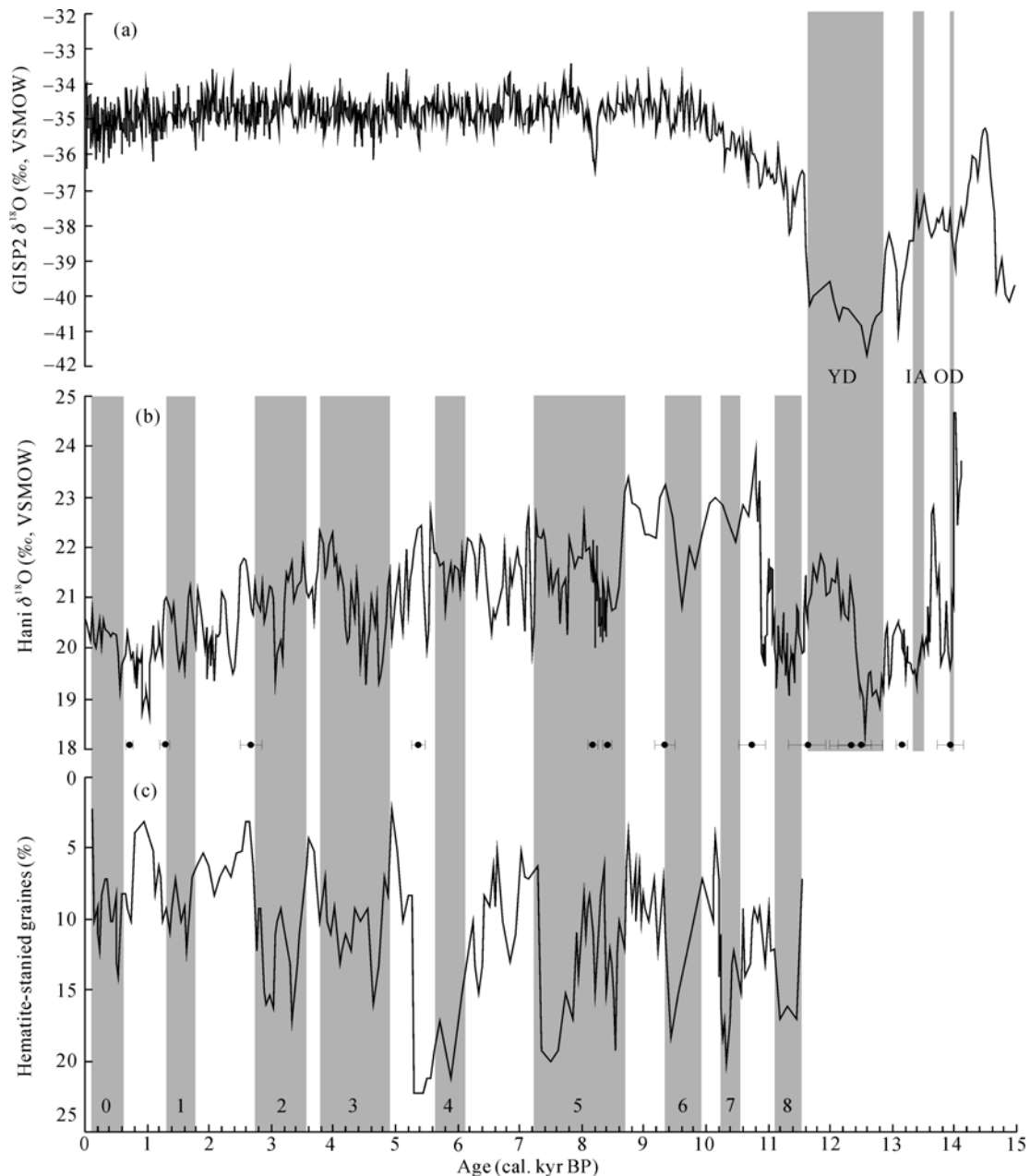


Figure 4 The $\delta^{18}\text{O}$ temperature proxy record of Hani peat cellulose (b) and its comparison with Holocene record of drift ice for the MC52-VM29-191 core in the North Atlantic (c)^[3] and the GISP2 $\delta^{18}\text{O}$ record (a) (<http://www.ncdc.noaa.gov/paleo/icecore/greenland/summit/document/gispisot.htm>) respectively. Numbers from 1 to 8 indicate the eight ice-rafted debris (IRD) events of the North Atlantic respectively^[3]. Number 0 indicates 'Little Ice Age' event^[3]. YD, IA, and OD denote the Younger Dryas, Inter-Allerød, and Older Dryas cooling events respectively^[11]. The vertical light grey bands trace the comparisons of temperature anomalies inferred from the Hani $\delta^{18}\text{O}$ with the cooling events. Black error bars show ^{14}C dates with 1σ error of the Hani peat profile (Table 2).

a number of sudden temperature drops are still indicated in the Western Pacific region, corresponding to a series of IRD events (IRD 7 to event 0) in the North Atlantic, respectively; however, as the Hani $\delta^{18}\text{O}$ record shows, these cooling events were primarily superimposed on a long-term warming trend. This pattern clearly differs from the abrupt temperature drop events of the last de-

glaciation that are superimposed on a long-term, generally colder tendency. Therefore, it may be favorable for recognition and contrast to take the cold peak time of another large-scale cooling event at about 11.3 cal. kyr BP, after YD event, as the starting point of Holocene.

It has been suggested that the warmest phase of the Holocene in the Chinese mainland, the so-called Holo-

cene Megathermal, was at around 8.5–3.0 kyr BP generally (^{14}C age), and different regions may have experienced different ages^[28,29]. For example, the Jinchuan peat and pollen record of Jinlin in the northeast of China is about at 10–3 kyr BP (^{14}C age)^[28,30]. Judged from the trend of average values ($\delta^{18}\text{O}$ was about 21‰), the Holocene Megathermal was at about 11–3 cal. kyr BP (Figure 4(b)), generally according with the climate status reflected by the Jinchuan pollen record.

The Holocene Megathermal reflected that the general climate status was warmer than nowadays. However, with improved sensitivity of proxy records and more in-depth investigation, researchers have paid more attention to abrupt climate events around the Holocene Megathermal on the centennial to millennial scales and studied its origin as well as its influence on human life. As mentioned above, the Hani record shows a series of abrupt climate change events that, superimposed over the Holocene Megathermal or even the whole Holocene, corresponded respectively with IRD events at nine time periods in the North Atlantic. The inference is that the repeated and abrupt climate anomaly during the interglacial period or warm period is a large-scale phenomenon, or at least a hemispheric phenomenon, which indicates that the distinct features of the Holocene climate were not stable.

3.3 The “8.2 kyr” event: a temperature anomaly of the early Holocene

The abrupt event about 8200 years ago is one of the most noticeable temperature anomalies in the Holocene because of its widespread distribution and assumed unique forcing mechanism. Observation and simulation studies suggest that at around 8.4 cal. kyr BP, a catastrophic meltwater discharge into the North Atlantic Ocean resulted in a slowdown of the North Atlantic Deep Water (NADW) formation and in reduced oceanic thermohaline circulation (THC), which, in turn, at around 8.2 cal. kyr BP led to the sharp temperature decrease in the Northern Hemisphere^[31,32]. Recently, based on the inference that the oldest age for the onset of the sharp cooling in the Greenland ice cores is near 8.3 cal. kyr BP, Rohling and Pälike^[33] argued that the sharp “8.2 k” event-itself triggered by the meltwater outburst-may be restricted to a much smaller (for example, North Atlantic) realm; in addition, they argued that many broad anomalies starting from about 8.3 cal. kyr BP ago seem related to solar output fluctuations.

The sensitive Hani $\delta^{18}\text{O}$ record provides the opportunity for a careful evaluation of the “8.2 kyr” event in the Western Pacific region. Figure 4(b) shows a broad $\delta^{18}\text{O}$ peak at about 8.3 cal. kyr BP. In addition, we found some concentrated areas of lower $\delta^{18}\text{O}$ values or a small sharp peak at around 8.2 cal. kyr BP in the Hani $\delta^{18}\text{O}$ curve. Further comparison with the residual atmospheric $\Delta^{14}\text{C}$ record^[34] reveals that from 8.6 to 8.2 cal. kyr BP, there are three declining $\delta^{18}\text{O}$ peaks in the Hani $\delta^{18}\text{O}$ record, and there are two ascending $\Delta^{14}\text{C}$ peaks and one falling peak in the $\Delta^{14}\text{C}$ record (Figure 5). The first $\delta^{18}\text{O}$ declining peak in the interval from about 8.6 to 8.48 cal. kyr BP shows a smaller, smoother temperature decrease, corresponding to the first $\Delta^{14}\text{C}$ rising peak indicating a smaller decrease of solar activity. The second declining $\delta^{18}\text{O}$ peak at around 8.41 to 8.25 cal. kyr BP shows a larger temperature decrease corresponding to the second larger $\Delta^{14}\text{C}$ rising peak, indicating a greater decrease in solar activity. Thus, the temperature variations within these two time intervals may be mainly related to reduced solar activity.

It is worth noting, however, that when the third $\delta^{18}\text{O}$ falling peak at 8.25 to 8.19 cal. kyr BP indicates a clear temperature decrease and the minimum is at around 8.22 cal. kyr BP, the $\Delta^{14}\text{C}$ record shows only a clearly decreasing peak, indicating increased solar activity. Obviously, this abrupt cooling, centered at around 8.22 ± 70 cal. kyr BP (Figure 5, Table 2), does not match the increased solar activity, but it closely parallels the sharp “8.2 kyr” event and should be considered as a meltwater-related cooling event in Northern Atlantic. The smaller amplitude of this cold event might be resulted from the balance of strengthened solar activity. Correspondingly, in the Hani peat profile there is a ~10 cm-thick greenish-grey clay peat deposition at a depth between 495 and 505 cm (Figure 3), possibly implying a lower temperature and drier environment unfavorable to vegetation development that may have resulted from relatively weaker activity of the East Asian summer monsoon inferred from the Hani peat $\delta^{13}\text{C}$ (by comparison with more stronger EAM during the period from around 8.4 to 8.3 cal. kyr BP^[5]). We conclude that the broad Hani $\delta^{18}\text{O}$ peak at around 8.3 cal. kyr BP genuinely reflects compound climate signals resulting from two kinds of forcing factors: reduced solar activity and the meltwater effect. The latter signal appears to provide paleo-temperature evidence for existence of the sharp

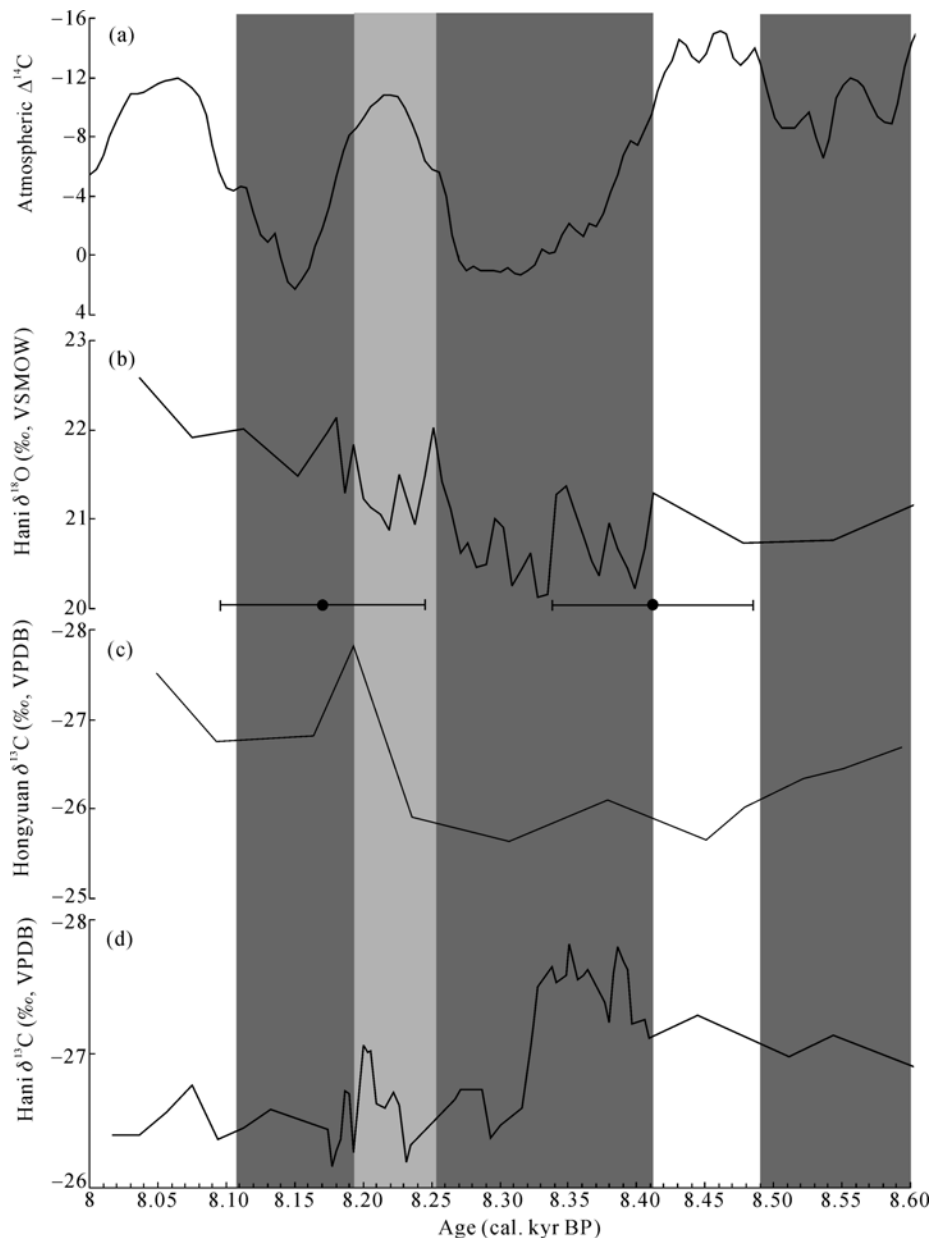


Figure 5 Interconnections between the surface temperature (b), Indian Ocean summer monsoon (c), East Asian summer monsoon (d), and solar activity (a) during the broad 8.2 kyr event. Three vertical grey bands trace interconnections between the reduced solar activity, decreased temperature, weakened ISM and strengthened EAM. The vertical light grey band traces un-matching relationship between the increased solar activity and decreased temperature. Black error bars show two ^{14}C dates with 1σ error of the Hani peat profile (Table 2).

“8.2 kyr” event in the western North Pacific region.

3.4 The “4.2 kyr” event: a temperature anomaly of the prehistoric period

A climate anomaly event that happened more than 4000 years ago in the late Neolithic period is a scientific problem that has attracted much attention. Some researchers call it the “4 kyr” event^[35,36] and others call it the “4.2 kyr” event^[4,37]. There are two differences between this event and the “8.2 kyr” event. First, human

civilization had not appeared when the “8.2 kyr” cooling event happened. The “4.2 kyr” event happened in the early stage of human civilization, and its influence on human civilization can be identified. Second, when the “4.2 kyr” event happened, the ice cap of the northern hemisphere had obviously retreated; therefore, the hypothesis that an outburst of meltwater brought on the reformation of ocean circulation for the “8.2 kyr” event is not applicable for the “4.2 kyr” event. Some studies have pointed out that a large-scale temperature decrease

happened at least in the northern hemisphere at about 4.2 cal. kyr BP, coupled with an abrupt change in the Asian monsoon that might have strongly influenced the development of ancient civilizations in different regions^[38]. When the temperature decreased at around 4.2 cal. kyr BP, the continual serious drought in the Indian summer monsoon region might have been connected with the collapse of the Akkadian Empire in west Asia and the decline of the early ancient Greek and Egyptian civilizations, as well as the decline of the Harappa civilization of the Indus Valley^[39–41]. In contrast, an abrupt strengthening of the East Asian monsoon with decreased temperature not only verifies the legend of a large floodwater event in the remote antiquity of China, but also possibly suggests important influences on the decline of the Longshan and Liangzhu cultures^[5,35,36,42]. Because the “4.2 kyr” event might have been the first serious natural catastrophe of continental scope after the appearance of human civilization, it shows the influence of abrupt climate anomaly changes (low temperature, drought, and floodwater) on human civilization, which has relevance for studying the adaptation of humans to global changes.

However, the signal year of the “4.2 kyr” event has not been determined. This not only induces different designations for the event but also impedes its identification from different proxy records and results in broad contrasts about the event. Now we can provide evidence to demonstrate that a temperature anomaly of the “4.2 kyr” event has a distinct difference from the “8.2 kyr” event. According to Figure 4, the event in the Northern Atlantic region is approximately equivalent to the IRD 3 events. Both the Hani $\delta^{18}\text{O}$ value and hematite-stained grains of ice raft demonstrate that over long periods of century or even nearly millennial scale, the air temperature in the two regions might have cooled repeatedly (at about 3.8 to 4.8 cal. kyr BP). The long-term temperature anomaly appeared obviously as a broad cool valley according to the Jinchuan peat $\delta^{18}\text{O}$ sequence and the Dunde ice core record^[20,28]. The activity change in the East Asian summer monsoon and Indian Ocean summer monsoon of the mid-low latitudes relatively and separately appeared as exceptional strength and decrease in this period^[4,5]. This change indicates that any long-term and recurrent event should be attended to when identifying and comparing “4.2 kyr” events in different proxy records and its impact on ancient civilization.

3.5 The Medieval Warm Period and the Little Ice Age

During the period from 900 A.D. to 1300 A.D., the temperature in the European region was distinctly higher, a time called the Medieval Warm Period. Because it is a distinct warm period nearest to the modern warming period and happened before the Industrial Revolution, it naturally becomes a comparison with modern warming. A universal concern in academic circles is whether it also existed outside the European region and whether it is a common phenomenon.

Chinese scholars believe that the Chinese mainland was distinctly warmer during the Medieval Warm Period in Europe. Investigation of heat-loving vegetables, such as mandarin oranges and ramie, in the subtropical zone in the same period of history, revealed that the scope of the north boundary of these crops at that time moved to the north of the Chinese mainland. It is estimated that the average temperature at that time was 0.9–1.0°C higher than modern temperatures^[43]. In recent years, based on the temperature rebuilding and simulation of phenological data of the history of east China^[44] and the research on climatic records of tree-rings in the west of China^[45], the temperature on the Chinese mainland was distinctly warmer during the Medieval Warm Period.

The above evidence is built on the basis of historic record and climatic records of tree-rings over quite a short time span. The peat cellulose $\delta^{18}\text{O}$ record over a long-term span also provides evidence that the Medieval Warm Period existed in the Chinese mainland. A peak value of $\delta^{18}\text{O}$ appeared at about 1.1 cal. yr BP in the Hani record. The increased $\delta^{18}\text{O}$ peak value is more distinct in the Jinchuan peat record, which is 15 km to the northwest of Hani^[20]. This difference may be related to the fact that the latter was developed based on a crater lake with a more stable sedimentary environment and a higher peat accumulation rate. It is important, however, that both the Hani and Jinchuan records demonstrate that the rise in air temperature indicated by the peat $\delta^{18}\text{O}$ value corresponding to the Medieval Warm Period is attributable to a long-term natural fluctuation of climate and corresponds well with obvious increases in solar activity at that time^[20,46].

A natural cooling, the so-called Little Ice Age, appeared after the above-described warm period. There are two cold peaks in the Hani $\delta^{18}\text{O}$ record at about 450 cal. yr BP and 250 cal. yr BP, and the first cold peat was the

most distinct. Both indicate two cold climate events of the Little Ice Age in the area, which is consistent with the Jinchuan peat $\delta^{18}\text{O}$ record and other proxy records as well as historic data^[20,29,46]. Both the Hani and Jinchuan peat $\delta^{18}\text{O}$ records show that the temperature in the district after the Little Ice Age gradually rose and became warmer in fluctuation.

The fact that these climate events appear in the Hani peat $\delta^{18}\text{O}$ record rather integrally contributes to recognition of the phenomenon of global climate change and relative response of regions. In addition to climate events of this kind, there is further information about climate change in the Hani peat $\delta^{18}\text{O}$ record. For example, at about 950 cal. yr BP, an abrupt cooling indicated by a small $\delta^{18}\text{O}$ value corresponded to the decline of the Mayan civilization in the Americas^[47]; at about 1.5 cal. kyr BP, a $\delta^{18}\text{O}$ cold peak tallied with an obvious decrease in temperature in the Northern-Southern Dynasties of China recorded in the historic literature^[48]; and at about 2.8 cal. kyr BP, a phenomenon of cooling down appeared in the northern hemisphere on a large scale^[49].

4 Conclusions

The time sequence of Hani peat cellulose $\delta^{18}\text{O}$ is a proxy indicator of sensitivity of the land surface tem-

perature. It comprehensively reproduces climate change events of different characters on the centennial to millennial scales recorded by indicators such as GISP2 $\delta^{18}\text{O}$ and ice raft of the Northern Atlantic. These include cooling events such as the Older Dryas, Inter-Allerød, Younger Dryas, and ice-rafted debris events at nine time points, as well as warming phenomena such as the Holocene Megathermal and the Medieval Warm Period.

This research reveals an important phenomenon in global change study, that is, the air temperature cooling pattern occurring repeatedly from the last deglaciation to the Holocene appeared not only in the northern Atlantic region but also in the northwest Pacific region of the middle latitudes. The result is significant for further exploration of the response of regional climate change to global change.

The swamp environment for peat growth and the physiological characteristics of the main plants composing peat have an important influence on the proxy temperature indicator for peat cellulose, $\delta^{18}\text{O}$. It not only allows Hani peat cellulose $\delta^{18}\text{O}$ to sensitively record the temperature of the land surface for a hundred years but also provides a comparison for peat cellulose ^{14}C age.

We thank three anonymous reviewers for their thoughtful reviews and suggestions.

- 1 Stuiver M, Grootes P M, Braziunas T F. The GISP2 $\delta^{18}\text{O}$ climate record of the past 16500 years and the role of the Sun, ocean, and volcanoes. *Quat Res*, 1995, 44: 341–354
- 2 Bond G, Showers W, Cheseby M, et al. A pervasive millennial-scale cycle in North Atlantic Holocene and glacial climates. *Science*, 1997, 278: 1257–1266
- 3 Bond G, Kromer B, Beer J, et al. Persistent solar influence on North Atlantic climate during the Holocene. *Science*, 2001, 294: 2130–2136
- 4 Hong Y T, Hong B, Lin Q H, et al. Correlation between Indian Ocean summer monsoon and North Atlantic climate during the Holocene. *Earth Planet Sci Lett*, 2003, 211: 371–380
- 5 Hong Y T, Hong B, Lin Q H, et al. Inverse phase oscillations between the East Asian and Indian Ocean summer monsoons during the last 12000 years and paleo-El Niño. *Earth Planet Sci Lett*, 2005, 231: 337–346
- 6 Yuan D X, Chen H, Edwards R L, et al. Timing, duration, and transitions of the last interglacial Asian monsoon. *Science*, 2004, 304: 575–578
- 7 Wang Y J, Chen H, Edwards R L, et al. The Holocene Asian monsoon: Links to solar changes and north Atlantic climate. *Science*, 2005, 308: 854–857
- 8 Qiao S Y. A preliminary study on Hani peat-mire in the west part of Changbai Mountain (in Chinese). *Sci Geograph Sin*, 1993, 13(3): 279–287
- 9 Green J W. Wood cellulose. In Whistler R L, ed. *Methods in Carbohydrate Chemistry*. New York: Academic Press, 1963. 9–22
- 10 Yapp C J, Epstein S. Climatic implications of D/H ratios of meteoric water over North America (9500–22000 B.P.) as inferred from ancient wood cellulose C-H hydrogen. *Earth Planet Sci Lett*, 1977, 34: 333–350
- 11 Barbour M M. Stable oxygen isotope composition of plant tissue: A review. *Funct Plant Biol*, 2007, 34: 83–94
- 12 Wershaw R L, Friedman I, Heller S J, et al. Hydrogen isotopic fractionation of water passing through trees. In: Hobson G D, Speers G C, Inderson D E, eds. *Advances in Organic Geochemistry. International Series of Monographs on Earth Sciences*. New York: Pergamon Press, 1966. 55–67
- 13 Dawson T E, Ehleringer J R. Streamside trees that do not use stream water. *Nature*, 1991, 350: 335–337
- 14 Libby L M, Pandolfi L J. Temperature dependence of isotope ratios in tree rings. *Proc Natl Acad Sci U S A*, 1974, 71: 2482–2486
- 15 Burk R L, Stuiver M. Oxygen isotope ratios in trees reflect mean annual temperature and humidity. *Science*, 1981, 211: 1417–1419
- 16 Ramesh R, Bhattacharya S K, Gopalan K. Climatic correlations in the stable isotope records of silver fir (*Abies pindrow*) trees from

- Kashmir, India. *Earth Planet Sci Lett*, 1986, 79: 66–74
- 17 Liu W G, Feng X H, Liu Y, et al. $\delta^{18}\text{O}$ values of tree rings as a proxy of monsoon precipitation in arid Northwest China. *Chem Geol*, 2004, 206: 73–80
 - 18 Anderson W T, Bernasconi S M, Mckenzie J A, et al. Model evaluation for reconstructing the oxygen isotopic composition in precipitation from tree ring cellulose over the last century. *Chem Geol*, 2002, 182: 121–137
 - 19 Bai G R, Wang S Z, Leng X T, et al. Bio-environmental mechanism of herbaceous peat forming (in Chinese). *Acta Geograph Sin*, 1999, 54(3): 247–254
 - 20 Hong Y T, Jiang H B, Liu T S, et al. Response of climate to solar forcing in a 6000-year $\delta^{18}\text{O}$ time series of Chinese peat cellulose. *Holocene*, 2000, 10: 1–7
 - 21 Yin S B, Liu X G. Discussion on “the theory on climate cause of peat forming” (in Chinese). *Sci Geograph Sin*, 2006, 26(3): 322–327
 - 22 Dansgaard W. Stable isotopes in precipitation. *Tellus*, 1964, 16: 436–468
 - 23 Gat J R. The isotopes of oxygen and hydrogen in precipitation. In: Fritz P, Fontes J C, eds. *Handbook of Environmental Isotope Geochemistry*. Amsterdam: Elsevier, 1980. 21–47
 - 24 Rozanski K, Araguas-Araguas L, Gonfiantini R. Relation between long-term trends of oxygen-18 isotope composition of precipitation and climate. *Science*, 1992, 258: 981–985
 - 25 Ménot-Combes G, Burns S J, Leuenberger M. Variations of $^{18}\text{O}/^{16}\text{O}$ in plants from temperate peat bogs (Switzerland): Implications for paleoclimatic studies. *Earth Planet Sci Lett*, 2002, 202: 419–434
 - 26 Stuiver M, Reimer P J, Bard E, et al. Radiocarbon calibration program rev 4.3. *Radiocarbon*, 1998, 40: 1041–1083
 - 27 Genty D, Blamart D, Ghaleb B, et al. Timing and dynamics of the last deglaciation from European and North African $\delta^{13}\text{C}$ stalagmite profiles—Comparison with Chinese and South Hemisphere stalagmites. *Quat Sci Rev*, 2006, 25: 2118–2142
 - 28 Shi Y F, Kong Z C, Wang S M, et al. The climatic fluctuation and important events of holocene megathermal in China. *Sci China Ser B*, 1992, 12: 1300–1308
 - 29 Wang S W, Gong D Y. Climate in China during the four special periods in Holocene (in Chinese). *Prog Nat Sci*, 2000, 10(4): 325–332
 - 30 Sun X J, Yuan S M. Vegetation evolution from pollen records in Jinchuan, Jilin Province in the past 10000 years. In: Liu T S, eds. *Loess · Quaternary Geology · Global Change*. Beijing: Science Press, 1990. 46–57
 - 31 Broecker W. Does the trigger for abrupt climate change reside in the ocean or in the atmosphere? *Science*, 2003, 300: 1519–1522
 - 32 Alley R B, Agústsdóttir A M. The 8k event: Cause and consequences of a major Holocene abrupt climate change. *Quat Sci Rev*, 2005, 24: 1123–1149
 - 33 Rohling E J, Pälike H. Centennial-scale climate cooling with a sudden cold event around 8200 years ago. *Nature*, 2005, 434: 975–979
 - 34 Reimer J, Baillie M G L, Bard E, et al. Residual delta ^{14}C around 2000 year moving average of IntCal04. *Radiocarbon*, 2004, 46: 1029–1058
 - 35 Xia Z K, Yang X Y. Preliminary study on the flood events about 4 ka B.P. in north China (in Chinese). *Quat Sci*, 2003, 23: 667–674
 - 36 Wu W X, Liu T S. Variations in east Asia monsoon around 4000 a B.P. and the collapse of Neolithic cultures around central plain (in Chinese). *Quat Sci*, 2004, 24: 278–284
 - 37 Staubwasser W, Sirocko F, Grootes P M, et al. Climate change at 4.2 ka BP termination of the Indus valley civilization and Holocene south Asian monsoon variability. *Geophys Res Lett*, 2003, 30: 1425–1428
 - 38 Hong B, Lin Q H, Hong Y T, et al. Interconnections between the Asian monsoon, ENSO, and high northern latitude climate during the Holocene. *Chin Sci Bull*, 2006, 51(18): 2169–2177
 - 39 Weiss H, Courty M A, Wetterstrom W, et al. The genesis and collapse of third millennial north Mesopotamian civilization. *Science*, 1993, 261: 995–1004
 - 40 Kutzbach J E. The changing pulse of the monsoon. In: Fein J S, Stephens P L, eds. *Monsoons*. New York: John Wiley & Sons, 1987. 247–269
 - 41 de Menocal P B. Cultural responses to climate change during the late Holocene. *Science*, 2001, 292: 670–673
 - 42 Yu W C. The secret for the decline of Liangzhu Culture and Longshan Culture (in Chinese). *Cultur Rel*, 1992, 3: 27–28
 - 43 Zhang D E. Evidence for the existence of the Medieval Warm Period in China. *Clim Change*, 1994, 26(3): 293–297
 - 44 Ge Q S, Zheng J Y, Liu J. Amplitude and rhythm of winter half-year temperature change in eastern China for the past 2000 years (in Chinese). *Adv Clim Change Res*, 2006, 2(3): 108–112
 - 45 Yang B, Kang X C, Shi Y F. Decadal climatic variations indicated by Dulan tree-ring and the comparison with the temperature proxy data from other regions of China during the last 2000 years. *Sci Geograph Sin*, 2000, 20(5): 397–402
 - 46 Liu J, Hans von Storch, Chen X, et al. Simulated and reconstructed winter temperature in the eastern China during the last millennium. *Chin Sci Bull*, 2005, 50(24): 2872–2877
 - 47 Hodell D A, Curtis J H, Brenner M. Possible role of climate in the collapse of Classic Maya civilization. *Nature*, 1995, 375: 391–394
 - 48 Zhu K Z. A preliminary study on the climatic fluctuations during the last 5000 years in China. *Sci China Ser A*, 1973, 16(2): 226–256
 - 49 Bas Van Geel, Johannes Van Der Plicht, Kilian M R, et al. The Sharp rise of $\delta^{14}\text{C}$ ca. 800 cal BC: Possible cause, related climatic teleconnections and the impact on human environments. *Radiocarbon*, 1998, 40(1): 535–550